AWS/TR--93/001

NEW TECHNIQUES for CONTRAIL FORECASTING

by

Capt Jeffrey L. Peters

AUGUST 1993

AIR WEATHER SERVICE
102 West Losey St
Scott Air Force Base, Illinois 62225-5206

REVIEW AND APPROVAL STATEMENT

AWS/TR--93/001, *New Techniques for Contrail Forecasting*, August 1993, has been reviewed and is approved for public release. There is no objection to unlimited distribution of this document to the public at large, or by the Defense Technical Information Center (DTIC) to the National Technical Information Service (NTIS).

WILLIAM S. WEAVING, Col, USAF
Air Weather Service Director of Technology

FOR THE COMMANDER

WALTER S. BURGMANN
Scientific and Technical Information
Program Manager
30 August 1993

The authors and editors of this publication welcome feedback, both positive and negative. We value your opinion. Please let us know what you like and do not like about our products. Also, please let us know if your address has changed, or if you wish to receive more or fewer copies of AWS and USAFETAC technical documents in primary distribution. If you need more copies of this document, or if you know of someone else who might be interested in this or other AWS/USAFETAC publications, let us know that too. Call, write, or FAX:

USAFETAC/DOL
859 Buchanan St
Scott AFB, IL 62225-5116

DSN 576-4044/2625/5023 Commercial 618 256-xxxx Fax 3772

REPORT DOCUMENTATION PAGE

2. Report Date: August 1993

3. Report Type: Technical report

4. Title: New Techniques for Contrail Forecasting

6. Authors: Capt Jeffrey L. Peters

7. Performing Organization Name and Address: HQ Air Weather Service, 102 West Losey St, Scott AFB IL 62225-5206

8. Performing Organization Report Number: AWS/TR-93/001

12. Approved for public release; distribution is unlimited

13. Abstract: This report documents the results of a study requested by the Strategic Air Command Deputy Chief of Staff for Operations (SAC/DO) to update previous contrail forecasting research done by Herbert Appleman for HQ Air Weather Service in 1953. Advancements in aircraft power plants, especially the development of bypass turbofan engines, made the new study necessary. This attempt to update and improve current contrail forecasting methods was performed by the SAC Directorate of Weather (SAC/DOW). It describes the development of new contrail forecast algorithms for several types of engines used in high-flying aircraft. It also provides contrail forecasting rules that correlate synoptic-scale upward vertical motion with contrail formation. The results indicate significant improvement in contrail forecasting accuracy over the Appleman technique now in use at the Air Force Global Weather Central.

14. Subject Terms: WEATHER, CLIMATOLOGY, CLOUDS, CIRRUS CLOUDS, FORECASTING, ALGORITHMS, CONDENSATION TRAILS, CONTRAILS, EXHAUST TRAILS, VAPOR TRAILS

15. Number of Pages: 37

17. Security Classification of Report: Unclassified

18. Security Classification of this Page: Unclassified

19. Security Classification of Abstract: Unclassified

20. Limitation of Abstract: UL

Standard Form 298

PREFACE

This report documents the results of a contrail study requested by the Strategic Air Command Deputy Chief of Staff for Operations. The study updates previous contrail forecasting research done by Herbert Appleman for HQ Air Weather Service in 1953. Advancements in aircraft power plants, especially the development of bypass turbofan engines, made the new study necessary.

This attempt to update and improve current contrail forecasting methods was performed by the SAC Directorate of Weather (SAC/DOW). The report describes the development of new contrail forecast algorithms for several types of engines used in high-flying aircraft. It also provides contrail forecasting rules that correlate synoptic-scale upward vertical motion with contrail formation. The results indicate significant improvement in contrail forecasting accuracy over the Appleman technique now in use at the Air Force Global Weather Central.

The author wishes to acknowledge the contributions of the USAF Environmental Technical Applications Center (USAFETAC); specifically, the Operations Applications Development Section of USAFETAC'S Aerospace Sciences Branch. USAFETAC/PR--92/003, *SAC Contrail Study*, by Capt Brian Bjornson, describes USAFETAC's considerable contribution to SAC/DOW's research and development of the new contrail forecasting techniques.

TABLE OF CONTENTS

FIGURES

TABLES

1. INTRODUCTION

Operational planners and pilots have been concerned about aircraft condensation trails (contrails) since World War II, for obvious reasons. Contrails provide the first visual clue that high-flying aircraft are approaching. Contrails are also used to locate aircraft from other aircraft or from satellites. To avoid the possibility that aircraft will be detected by their contrails, mission planners can make adjustments to flight levels or routes for a given mission based on an accurate contrail formation forecast and minimize the chances for detection, especially at critical mission points.

Air Weather Service (AWS) has understood the importance of contrail forecasts for some years. A series of contrail formation studies was begun in the 1950s. The results were presented in numerous AWS Technical Reports, most by Appleman (1953), whose work advanced that of Goldie (1941a, b) and Dobson (1941). Appleman derived contrail formation curves that allowed for a graphic method of forecasting contrails. This method, shown in Figure 1, uses a nomogram with ambient pressure, relative humidity, and temperature as forecast variables. If the forecaster knows the proposed flight level of the aircraft, as well as the relative humidity and temperature at flight level, a "yes/no" contrail forecast is possible.

In 1989, the Strategic Air Command Deputy Chief of Staff, Operations (SAC/DO), expressed concern with the accuracy of the contrail forecasts SAC aircrews were receiving. A subsequent USAFETAC study (Miller, 1990) showed the current AWS contrail forecasting algorithm to have poor skill. Concern from the operational community led the SAC Directorate of Weather (SAC/DOW) to initiate the contrail formation study described here. USAFETAC continued to support SAC/DOW efforts with statistical analysis of new data (Bjornson, 1992).

This report documents the capability of the current Air Force Global Weather Central (AFGWC) contrail forecast model and develops a better understanding of contrail formation as it relates to large-scale weather patterns. Contrail forecasting rules that correlate synoptic-scale vertical motion with contrail formation are also presented, along with new contrail forecasting algorithms for three aircraft engine categories: non-bypass turbojet, low-bypass turbofan, and high-bypass turbofan.

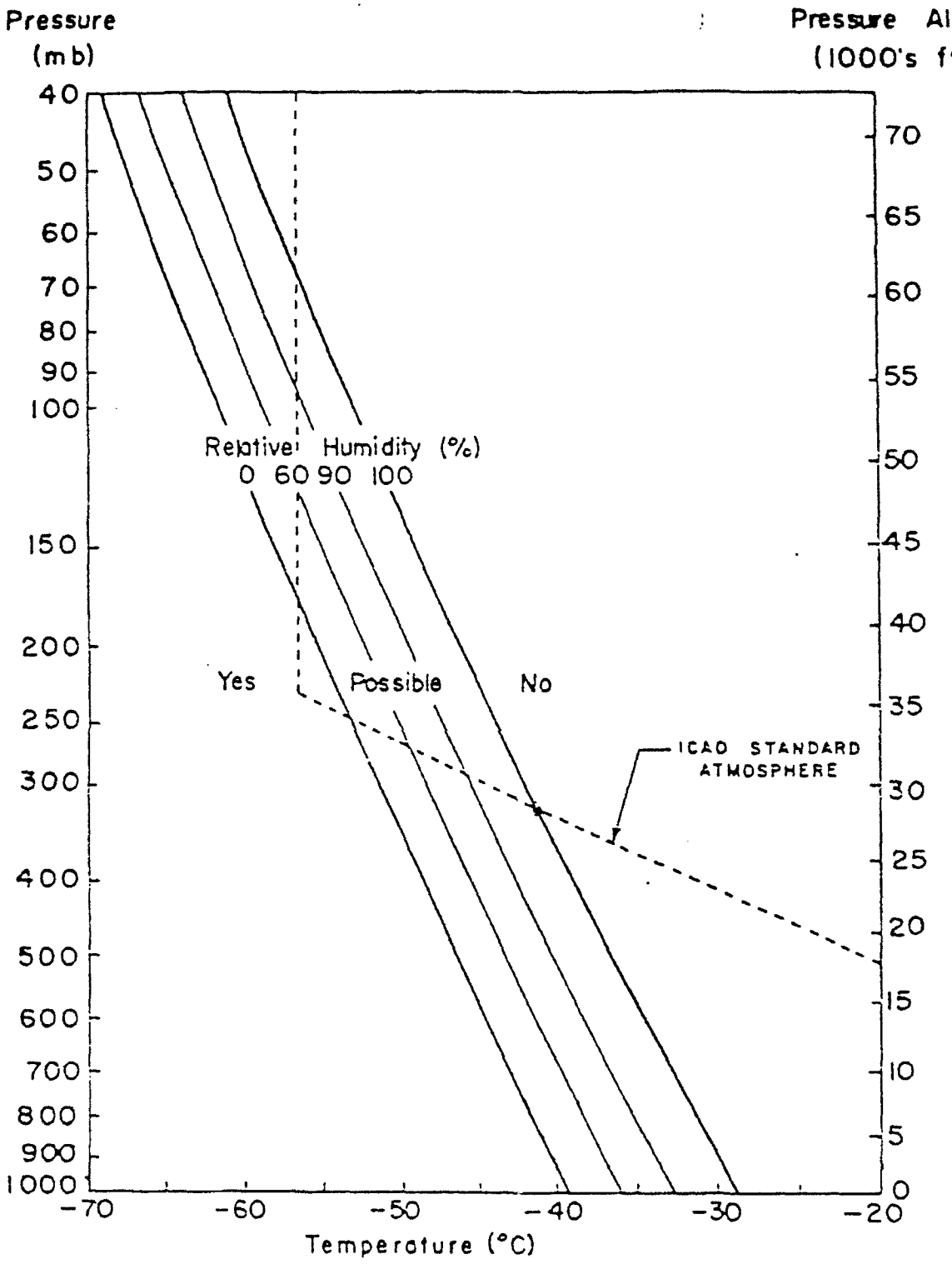

Figure 1. The Appleman Contrail Forecast Nomogram (1953).

2. PREVIOUS CONTRAIL FORECASTING RESEARCH

Goldie (1941a) investigated the formation of clouds behind aircraft (contrails) and identified several factors that encouraged their formation. Among those factors were water vapor and condensation nuclei produced by the combustion of aviation fuel. Conversely, Goldie found that heating from engines and propellers tended to *prevent* contrail formation. Based on his findings, Goldie suggested two operational tactics for avoiding the formation of contrails. First, pilots should avoid levels at which cirrus clouds are visible. Second, if contrails are present and the air is drier above, the pilot should climb. Goldie also presented a contrail forecasting aid, derived from Spitfire III engine data, that gave meteorologists and pilots an indication of flight levels at which contrails might form.

Dobson (1941) also used data from the Spitfire III study to produce a graph that showed the relationships of temperature, relative humidity, contrail cross-section, and aircraft power setting. Dobson concluded that contrails are possible when-ever cirrus is expected and temperature is below -53° C at cirrus height.

Appleman (1953), however, did the most extensive work ever attempted on the subject of contrail formation, using simple mixing cloud theory to represent contrail formation. For example, he represented the change in moisture and temperature in the aircraft's wake as $\Delta w/\Delta T$ (change in mixing ratio/change in temperature); this ratio is called the "critical slope." It represents the mixing of the engine exhaust with the environment. Appleman computed a critical slope value of 0.0336g/kg° C. His work resulted in a contrail forecast nomogram (Figure 1) that used ambient pressure, relative humidity, and temperature as forecast variables.

Appleman's first contrail forecasting technique was based on these assumptions:

- That saturation with respect to water is required.

- That after water droplets form, immediate freezing will occur.

- That an ice crystal content of 0.004 g/m^3 is required for a visible contrail.

Jiusto and Pilie (1964) gave a complete description of contrail forecasting and visibility, including the dependence of contrail visibility on viewing angle. They also stated that Appleman's 1953 graphic forecast method could be used, but with a few qualifications. Jiusto and Pilie advanced contrail forecasting by first establishing a relationship between synoptic-scale vertical motion and contrail formation and by developing engine-specific contrail forecast algorithms.

By the late 1980s, the quality of operational contrail forecasts (which still used the basic Appleman technique), was questioned by the SAC Director of Operations. After a USAFETAC study (Miller, 1990) confirmed that the current method had little skill, SAC/DOW continued to work on methods that would determine the *moisture* input variable more accurately and submitted the resulting new method (which included an engine-specific factor) to USAFETAC for evaluation and discriminant analysis. The new engine-specific contrail forecasting algorithms were supported by USAFETAC's empirical curves (Bjornson, 1992). When moisture data is missing, it was found that the RH profile should be assumed to be 60% in the troposphere and 20% in the stratosphere.

3. CONTRAIL FORMATION

Appleman (1953) and Jiusto and Pilie (1964) represented a contrail as a "mixing cloud," which forms when two parcels of air mix and become supersaturated with respect to water; the formation of water droplets is the result. This process is shown in Figure 2.

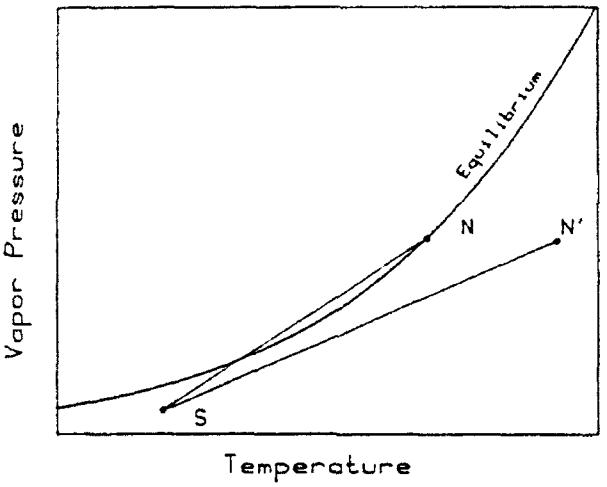

Figure 2. The Formation of a "Mixing Cloud."

An unsaturated mixture is represented by the two parcels, S and N'. The resulting mixture of S and N' is represented by the line between the two points. Since this line never crosses the saturation vapor pressure curve, a cloud will not form. But since the line representing the *mixing* of parcels S and N *does* cross the saturation vapor pressure curve, the mixture becomes supersaturated with respect to water and a cloud forms. In the case of a contrail, the "mixture" is composed of the engine exhaust gas and the ambient air.

Using mixing cloud theory, contrail forecasting depends on an accurate representation of ambient air conditions, as well as the temperature and moisture content of the engine exhaust gas. These variables are referred to as "initial conditions."

Figure 3 shows how knowledge of the initial conditions lead to an accurate contrail forecast. Three examples are shown using the same aircraft engine exhaust temperature and moisture content (represented by point A) and three different ambient air conditions represented by points B, C, and D.

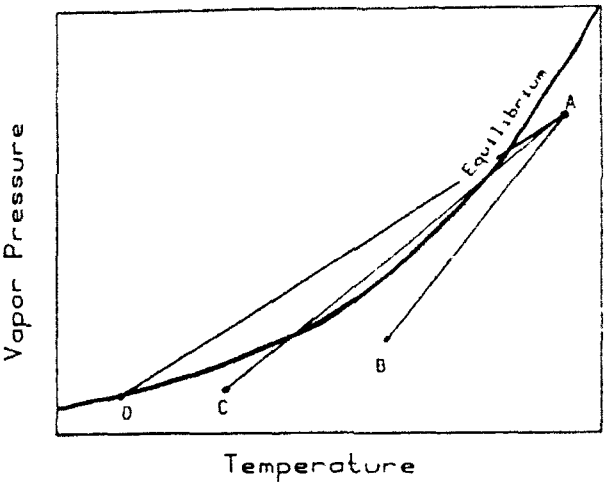

Figure 3. Mixing Engine Exhaust and Environmental Air.

When A and B mix, the mixture never becomes supersaturated with respect to water; contrails will not form. The mixing of A and C results in supersaturation; a contrail *will* form. The mixture of A and D results in a saturated condition. Since D was already saturated, will a contrail form? From the author's personal observation of contrails forming in cirrus decks, he believes that the A-D mixture *would* result in a contrail.

If we treat contrails as a mixing cloud and assume that they form only when the mixture of engine exhaust and ambient air reaches saturation, contrail forecasting would be a relatively simple matter. Obtaining the initial conditions along a given route, however, is neither easy nor

simple. Some averaging, then, must be done to simplify the forecast scheme.

Appleman (1953) introduced the concept of a "critical slope" to simplify contrail forecasting. The critical slope is simply the ratio of exhaust moisture to exhaust temperature. Figure 4 is an example of how critical slope is used to forecast contrails.

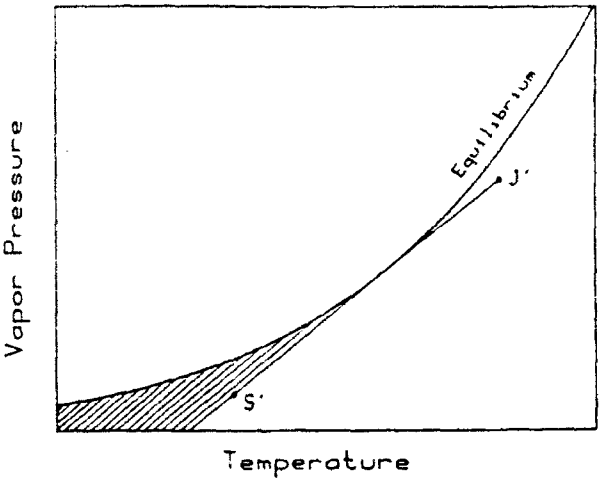

Figure 4. Critical Slope in Contrail Forecasting.

Point J' represents engine exhaust gas. The line from J' through S' represents the critical slope. If the ambient condition is in the shaded area, the mixture becomes supersaturated at some point and a contrail will form. If the ambient condition is to the right of the critical slope, a forecast of "no contrail" is indicated.

The critical slope calculated by Appleman (1953) was based on the amount of energy and moisture added to the engine exhaust gas by the combustion of aircraft fuel. Appleman determined this value to be 0.0336 g/kg° C. Because his research was conducted well before the development and general use of the turbofan engine, an update was required.

New critical slopes for the three most common engine categories (non-bypass turbojet, low-bypass turbofan, and high-bypass turbofan) are given in Chapter 6. Derivation of the new critical slopes was based on the assumption that the fuel-to-air ratio for each category of engine is significantly different.

4. CONTRAIL FORMATION AT OR BELOW 40,000 FEET

Since our analysis indicated that present forecast methods *underforecast* contrail formation below 40,000 feet, but *overforecast* contrails above 40,000 feet, the study was conducted in two parts; one used data from at or below 40,000 feet, the other from above 40,000 feet.

For the study of contrail formation at and below 40,000 feet, contrail observations were collected from SAC KC-135, RC-135, EC-135, B-1B, and B-52 aircraft from 1 May 1990 to 30 April 1991. Aircrews reported time and date of observation, pressure altitude, corrected outside air temperature, latitude, longitude, and contrail condition.

The 1-year data collection effort resulted in a database that contained 4,387 observations below 40,000 feet. Figure 5 shows the geographic distribution of all contrail reports collected below 40,000 feet.

As shown in the figure, the data was widely distributed, but the highest concentration of reports was over California. Although the data was collected over the United States, the results of the analysis should apply worldwide; contrail formation depends purely on exhaust gas characteristics, flight level, and the ambient temperature and relative humidity.

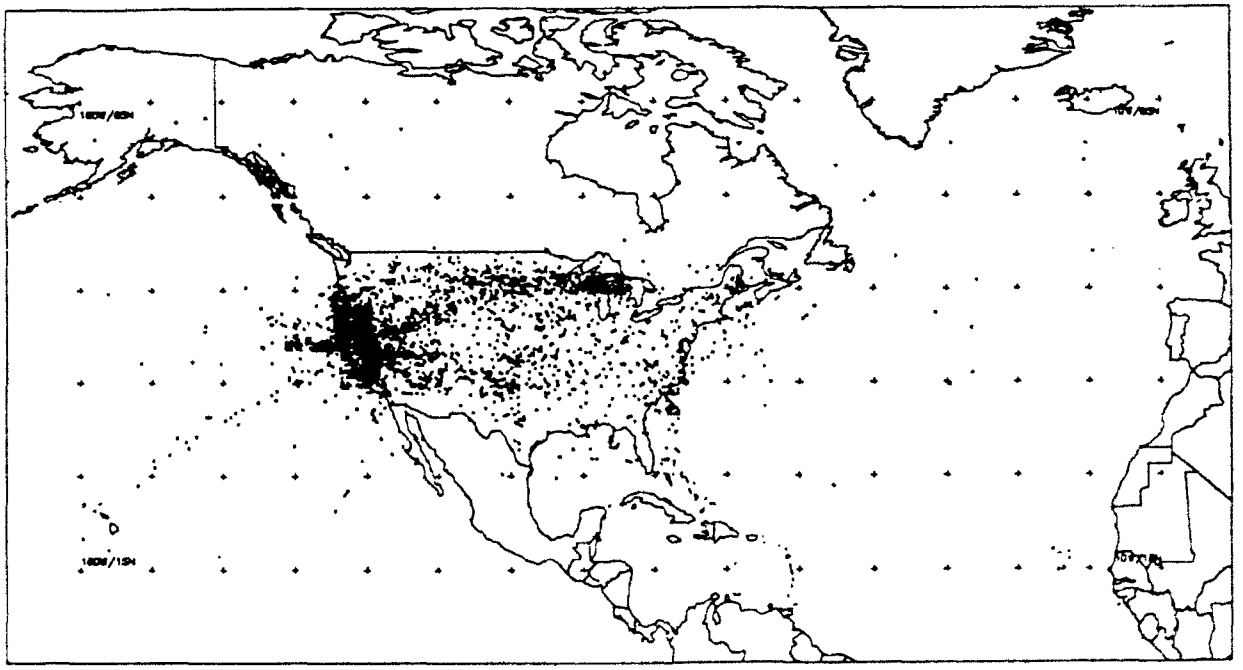

Figure 5. Geographic Distribution of Contrail Reports at and Below 40,000 Feet. The database contained 4,387 reports, most from over the western United States (Bjornson, 1992).

All reports were reviewed for meteorological consistency. If the pressure altitude and the outside air temperature were not consistent, a dry adiabatic assumption (combined with use of the standard atmosphere for altitude) was used to correct the temperature. The 300-mb chart that best coincided with the report time was most often used as an initial reference point for the temperature correction when needed.

All data was analyzed for correlations and sensitivities using temperature, altitude, vertical motion, and combinations of the three as key elements. The sign of the vertical motion (+ or -) was estimated, using the 300-mb trough or ridge pattern. Upward motion was assumed to exist between the base of a trough and the apex of the upstream ridge. Downward motion was assumed between the apex of the ridge and the base of the upstream trough.

A simple statistical analysis was conducted in an attempt to further our basic understanding of contrail formation. We started by analyzing all 4,387 contrail reports collected at or below 40,000 feet. The total number of contrail occurrences was 1,121, or 25.5% of observations. Non-occurrences were reported in 3,266 reports, or 74.5%.

Figure 6 shows that the percent occurrence frequency of contrails increases from near zero at 15,000 feet to near 85% at 39,000 feet. But the seasonal data (not shown) suggests that the percent frequency of contrails at lower altitudes is greater in winter and spring than in summer and fall. The percent frequency of contrails at a given altitude, on the other hand, varies considerably with location because contrail formation is highly dependent on ambient temperature.

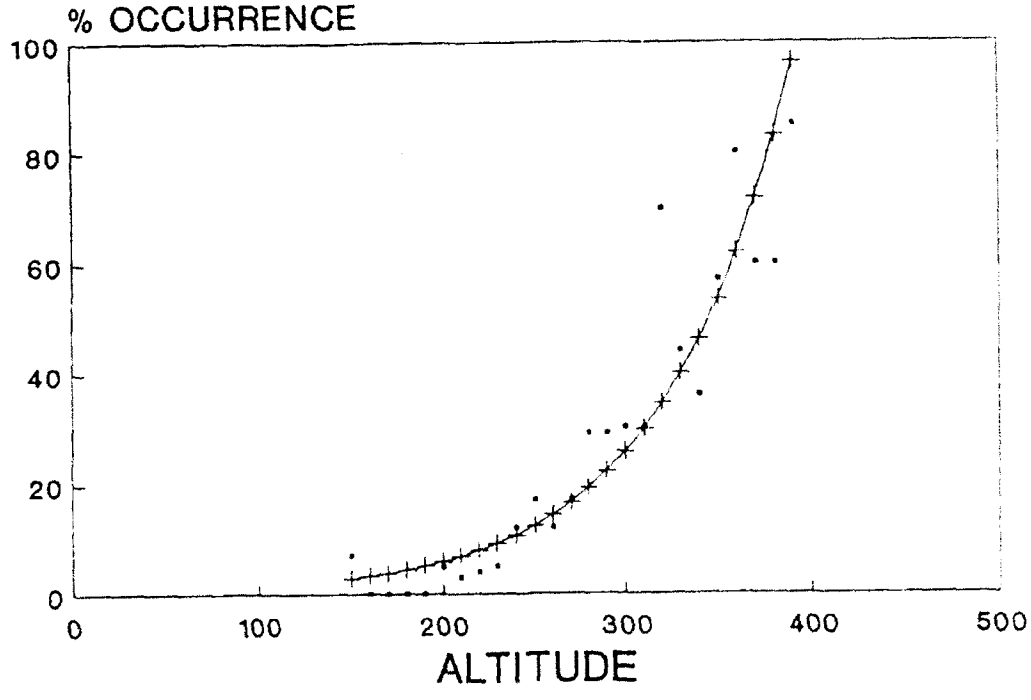

Figure 6. Contrail Percent Occurrence Frequency as a Function of Altitude.

The results of our temperature analysis are shown in Figure 7. They show that contrails form at temperatures as high as -10° C. This agrees with Rangno and Hobbs (1983) who reported the presence of "aircraft-produced ice particles" in clouds with temperatures of -8° C. As the temperature decreases, the frequency of contrails increases slowly from 8% in the -20 to -29° C range to 12% in the -30 to -39° C range.

As temperature continues to decrease, the frequency of contrail occurrence increases dramatically, reaching 73% at -51° C. Below -51° C, frequency remains above 70%. From Figure 7, the range of -49° C ≤ T ≥ -40° C is the transition zone from *favorable* to *unfavorable* contrail formation conditions. Since many military aircraft operate in this range, the ability to forecast contrails there is critical.

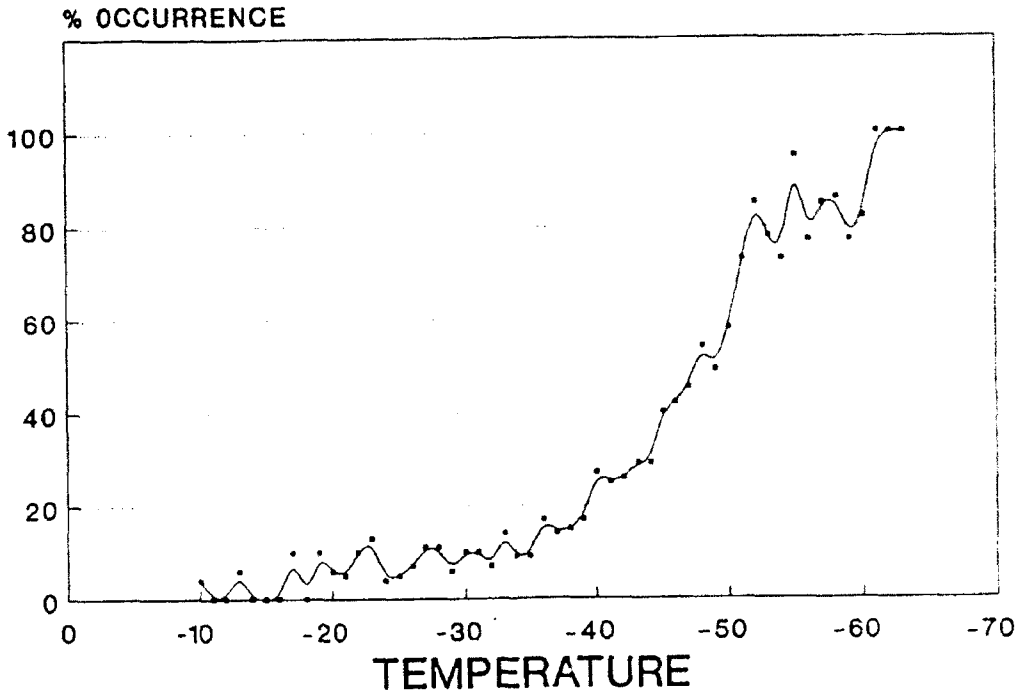

Figure 7. Contrail Percent Occurrence Frequency as a Function of Temperature.

The correlation between contrail occurrence and vertical motion was also analyzed closely, with the assumption that since synoptic-scale upward vertical motion produces the saturation vital to the formation of clouds, it would also be important to contrail formation. The sign of the vertical motion was estimated using the 300-mb trough-ridge pattern. Table I shows the sensitivity of contrail formation to vertical motion.

TABLE 1. Contrail Formation Sensitivity to Vertical Motion. As shown, the chances for contrail formation increase drastically when upward motion occurs in either of the three temperature categories.

	-39°≤T≤-30°	-49°≤T≤-40°C	T≤-50°C
Upward Motion and Occurrence	126	381	185
Upward Motion and Non-Occurrence	640	338	36
Downward Motion and Occurrence	43	142	150
Downward Motion and Non-Occurrence	563	652	226
Upward Motion and Occurrence/Total OBS with Upward Motion	126/766 16%	381/719 53%	185/221 84%
Downward Motion and Occurrence/Total OBS with Downward Motion	43/606 7%	142/794 18%	150/226 66%

For temperatures higher than -50° C, the table shows a large increase in contrail frequency with synoptic-scale upward motion. This correlation between vertical motion and contrail occurrence indicates the importance of relative humidity in contrail formation. For temperatures between -30 and -39° C, the 16% frequency of occurrence with upward motion shown in Table 1 is only slightly higher than when considering temperature alone as a forecast input variable. Between -40 and -45° C, 29% of the observations had contrail occurrences, and 46% of those were associated with upward motion.

Similarly, the contrail frequency for the -49°≤T≤-46° C category was 48%; 73% were associated with upward motion. At or below -50° C, vertical motion is not as important as a discriminator in contrail formation.

From this analysis, it is apparent that vertical motion has potential as a forecast variable in the -49°≤T≤-40° C range. Chapter 8 outlines more details of the vertical motion/contrail formation relationship when coupled with engine-specific algorithms.

5. CONTRAIL FORMATION ABOVE 40,000 FEET

For the portion of the study that considered contrail formation above 40,000 feet, contrail observations were collected by U-2 and TR-1 aircraft from May 1990 to August 1991. Pilots reported time, date, pressure altitude, corrected outside air temperature, latitude, longitude, and contrail condition. The effort resulted in a database of 1,040 observations, 61% of which reported contrail occurrence. As before, the data was analyzed for trends and sensitivities, using temperature and altitude.

Although the higher altitude data collection was from a comparatively small geographical region, the results can be transferred to other regions with a few adjustments. The most significant geographical variable appears to be the height of the tropopause, which is important because of the decreased moisture and different temperature profile in the stratosphere. The data used in this study was collected in an area where the average tropopause height was about 54,000 feet.

Although the small data collection area was relatively small, knowledge of the tropopause height in the area of interest minimizes the problem.

Other (and perhaps more important) limitations in reporting contrails above 40,000 feet include the limited ability of pilots to see non-persistent or thin contrails. U-2 pilots in particular may not have been able to see contrails (especially non-persistent contrails) because it is difficult to see directly behind the aircraft. In at least one case, the pilot of an AWACS aircraft reported a persistent contrail behind a U-2 when the U-2 pilot could not see it. The detection of contrails at different view angles is discussed by Jiusto and Pilie (1964).

We performed a simple statistical analysis of the high-altitude data in an attempt to further the understanding of high-altitude contrail formation. The temperature data showed a 24% frequency of occurrence of contrail formation in the $-66° \leq T \leq -60°$ C category, and a 66% frequency for the $-69° \leq T \leq -67°$ C category. For $T \leq -70°$ C, the frequency was 92%. The altitude data indicated an 82% contrail formation frequency at or below 63,000 feet, falling sharply to only 37% above 63,000 feet. This sharp decline appears to be the result of the drier and warmer stratospheric moisture and temperature profile in the data collection area.

6. VERIFICATION STATISTICS

The Air Force Global Weather Central (AFGWC) 18-hour contrail forecast model and the Appleman (1953) contrail forecast graph shown in Figure 1 were both verified as part of this study. The AFGWC 18-hour forecast model uses the Appleman forecast method, but with forecast temperatures and *assumed* relative humidities. The Appleman method can use either forecast or observed data. For this study, the Appleman method was verified using observed temperatures and relative humidity assumptions of 40% in the tropopause, 70% near the tropopause, and 10% in the stratosphere.

Table 2 shows the results of this analysis for data at or below 40,000 feet. As shown in the table, the POD (probability of detection) is the ratio of correct forecasts to the number of times the event occurred. The FAR (false alarm rate) is the ratio of incorrect forecasts to the number of times the event was forecast. Hanssen and Kuipers (1968) developed the discriminant "V" score (VDS), which gives an impartial measure of forecast accuracy by using a 2 by 2 matrix. The range of the VDS is from -1 (no skill) to 1 (perfect skill).

TABLE 2. Verification Statistics: The Appleman Method Vs AFGWC's 18-Hour Forecast at or Below 40,000 Feet.

	OCCURRENCE		NON-OCCURRENCE		
	POD	FAR	POD	FAR	VDS
APPLEMAN	27%	20%	98%	20%	0.25
GWC	24%	18%	98%	21%	0.22

For data at or below 40,000 feet, the Appleman method correctly forecast 3,199 non-occurrences out of 3,277 chances, for a POD of 98%. The AFGWC 18-hour forecast model forecasted 2,664 non-occurrences correctly out of 2,714 chances, also giving a POD of 98%. The verification of occurrences, however, was much worse. The Appleman method correctly forecast 305 occurrences out of 1,125 chances for a POD of only 27%. The AFGWC 18-hour forecast model forecast 225 occurrences out of 930 chances for a POD of only 24%.

The Appleman method, then, is shown to severely *underforecast* contrail occurrences at or below 40,000 feet.

On the other hand, the VDS for the Appleman method (0.25) and AFGWC forecast (0.22) showed at least some skill at or below 40,000 feet. The skill shown, however, was so low that the search for other, better, contrail forecasting schemes continued. Chapters 6 and 7 describe those new techniques and their development.

Table 3 shows the results of the verification for data *above* 40,000 feet. The Appleman method correctly forecast 190 occurrences of 407 chances, for a POD of 47%; the AFGWC model had a POD of 80%. Occurrence verification for the Appleman method was 601 occurrences forecast out of 633 chances, for a 95% POD. The AFGWC model forecast 209 occurrences out of 327 chances, for a 64% POD.

The Appleman method, then, *underforecasts* non-occurrences above 40,000 feet, the opposite of its performance below 40,000 feet. The VDS for both Appleman and AFGWC is significantly higher above 40,000 feet, but the lack of skill in forecasting non- occurrence shows that improvement is needed. The next few chapters describe new algorithms for high-altitude contrail forecasting.

TABLE 3. Verification Statistics: The Appleman Method Vs AFGWC's 18-Hour Forecast above 40,000 Feet.

	OCCURRENCE		NON-OCCURRENCE		
	POD	FAR	POD	FAR	VDS
APPLEMAN	95%	27%	46%	12%	0.42
GWC	64%	16%	80%	43%	0.43

7. ENGINE-SPECIFIC ALGORITHMS

Appleman (1953) developed his contrail forecasting method by using the ratio of moisture to energy released by the combustion of jet fuel, then converting that relationship to a mixing ratio to temperature ratio. As given earlier in this report, this value ("critical slope") was 0.0336 g/kg° C. Knowing the critical slope makes it possible to produce the contrail forecast method shown in Figure 1. The physics behind the basic method for forecasting contrails (the mixing cloud theory) was discussed in Chapter 2. However, the verification statistics in Tables 2 and 3 suggest that the critical slope value of 0.0336 g/kg° C is inadequate for the jet engines in use today. Working from this hypothesis, new contrail forecast algorithms for three classes of jet engines were investigated.

Engine characteristic data for a non-bypass turbojet and for low- and high-bypass turbofan engines were obtained from United Technologies/Pratt & Whitney. Engine exhaust characteristics (tailpipe moisture and temperature) were obtained for a wide range of power settings, Mach numbers, and flight levels.

New critical slopes were then calculated for various flight levels and compared to Appleman's. In Table 4, the new values for 35,000 feet are compared to Appleman's original.

TABLE 4. Critical Slope Comparison at 35,000 Feet.

Appleman	0.0336 g/kgC
Non-bypass	0.0360 g/kgC
Low-bypass	0.0400 g/kgC
High-bypass	0.0490 g/kgC

The result is a significantly different critical temperature (the temperature at which contrails will form at a given flight level and relative humidity) for each of the three engine types. The critical slope was not only different for each engine type, but it changed slightly with flight level for each engine type. By combining critical slopes and saturation vapor pressure curves (as shown in Figure 2), critical temperatures were obtained for various flight levels and relative humidities. Critical temperatures derived at various flight levels were used to obtain additional critical temperatures by interpolation. The resulting critical temperatures for each of three Pratt & Whitney jet engines are given in Figure 8 (non-bypass turbojet PWJ75), Figure 9 (low-bypass turbofan PWTF33), and Figure 10 (high-bypass turbofan PWF117). These results are significantly different from the original Appleman nomogram in Figure 1.

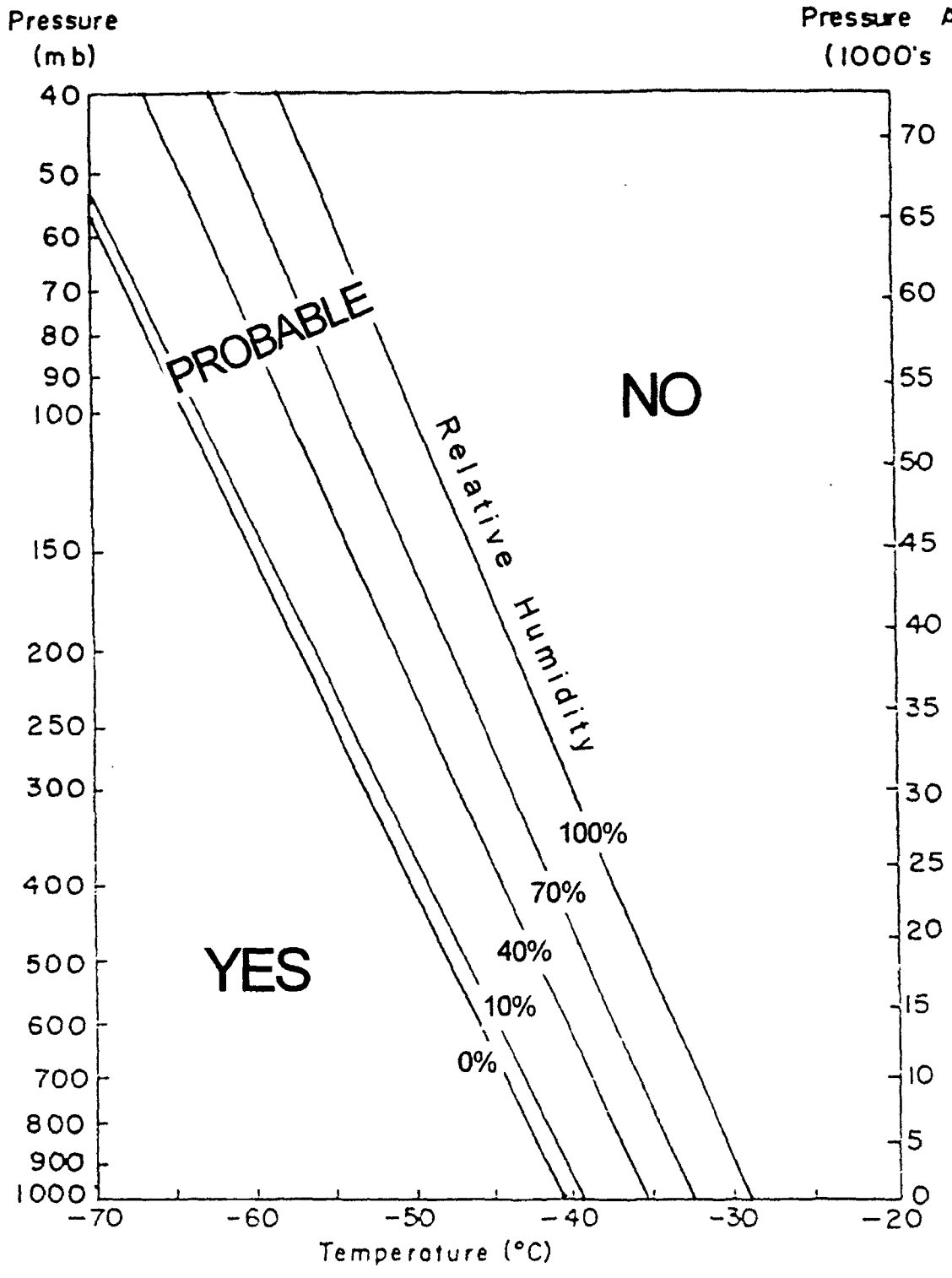

Figure 8. Non-Bypass Engine Contrail Algorithm.

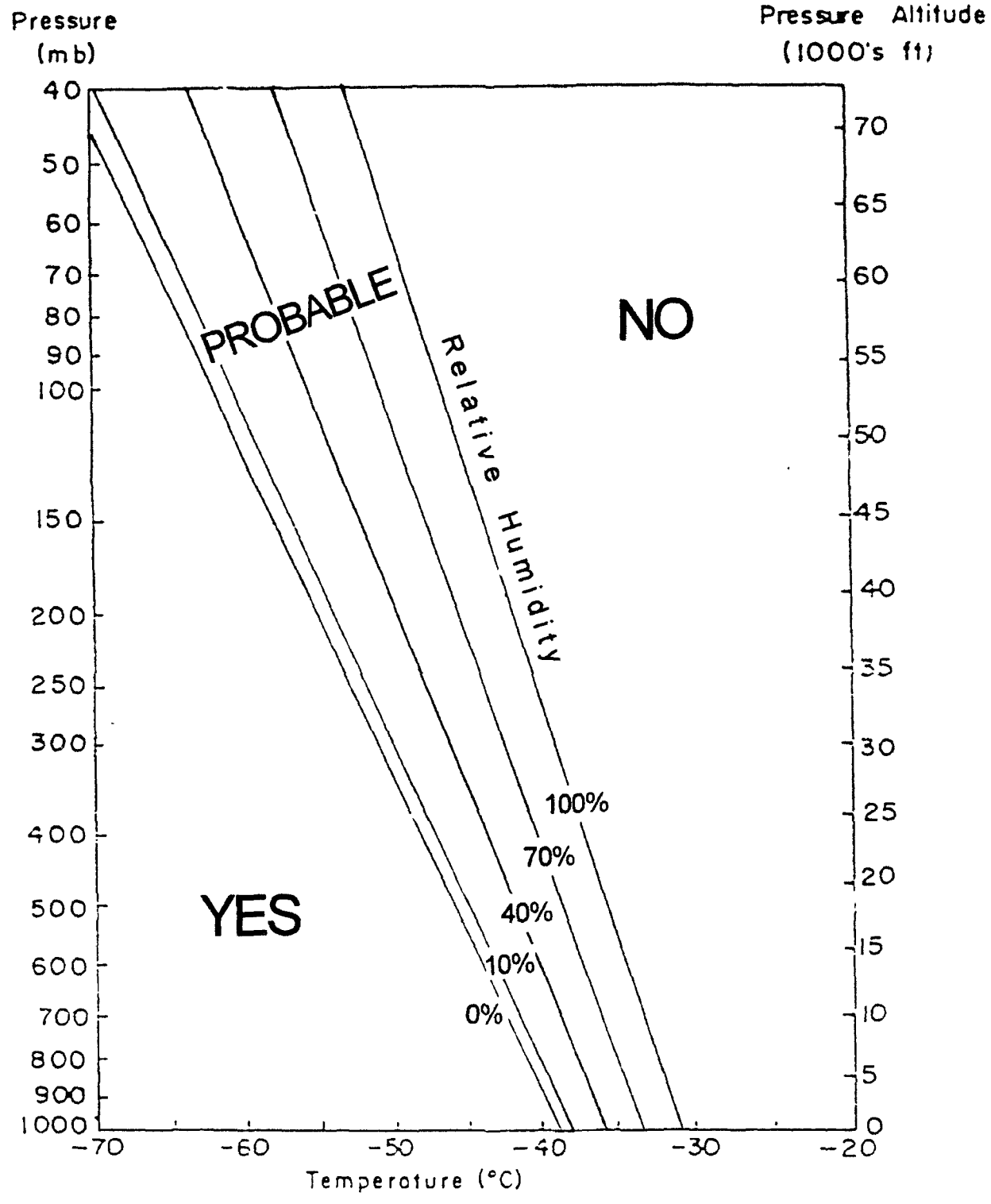

Figure 9. Low-Bypass Engine Contrail Algorithm.

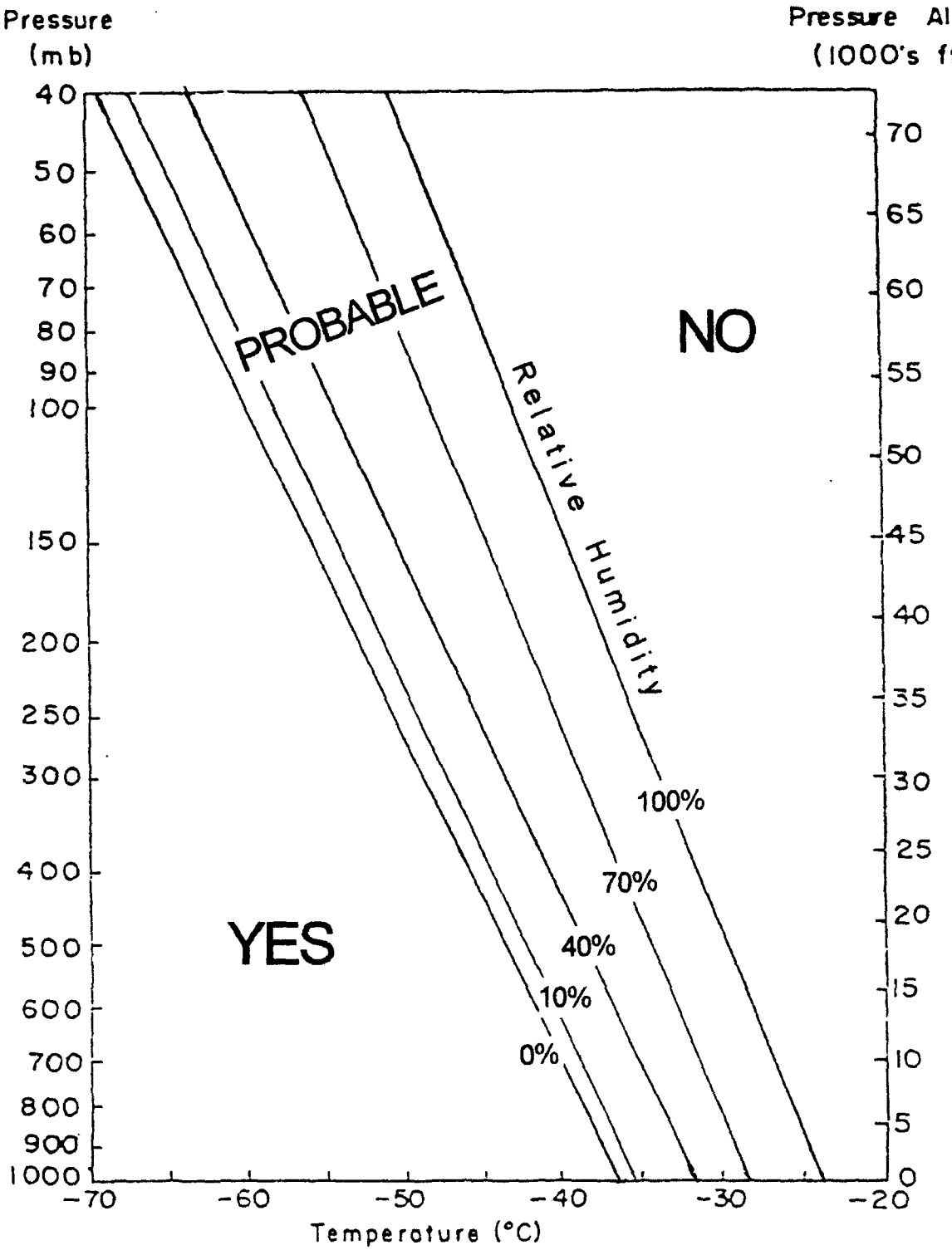

Figure 10. High-Bypass Engine Contrail Algorithm.

There are, or course, other jet engines with different critical temperatures than the ones shown here. If these temperatures are not adequate to support your customers, you can create your own forecast algorithms by obtaining tailpipe temperature and mixing ratio data for a range of power settings, Mach numbers, and flight levels. This data is available from your local engine maintenance people. Once you have it, simply calculate a critical slope for each flight level, as shown here. First, convert the mixing ratio to vapor pressure as shown in Equation 1.

$$e = \frac{wp}{622w} \tag{1}$$

Where w is the mixing ratio, p is the ambient pressure and e is the vapor pressure. Now take the ratio of vapor pressure (e) to temperature (T). This number will be your critical slope, expressed in terms of vapor pressure.

Next, find the temperature at which your critical slope is tangent to the saturation vapor pressure curve. This is done by taking the derivative with respect to temperature of the saturation vapor pressure form of Equation 2 (Equation C-2(C), AWS/TR-83/001).

$$e_s = 10^{\left[3.5665\log_{10}(T) - 0.0032098T - \left(\frac{2484.956}{T}\right) + 2.0702294\right]} \tag{2}$$

Where e_s is the saturation vapor pressure and T is the ambient temperature.

Now take the derivative with respect to temperature of Equation 2.

$$s = 10^{\left[3.5665\log_{10}(T) - 0.0032098T - \frac{2484.956}{T} + 2.0702294\right]} \log_e(10) \times Y$$

$$\text{where: } y = \left[3.56654\left(\frac{1}{T}\right)\log_{10}(e) - 0.0032098 + \frac{2484.956}{T^2}\right] \tag{3}$$

Where e is the exponential function and s is the critical slope. After you take the derivative, place temperatures in the resulting equation until you find the temperature that allows the resulting equation to equal the critical slope. This temperature is the critical temperature at 100% relative humidity for that particular flight level. The critical temperature for zero relative humidity, $T_c(0)$, can be calculated by dividing the saturation vapor pressure at $T_c(100)$ by the critical slope and subtracting the result from $T_c(100)$, as shown in Equation 4.

$$T_c(0) = T_c(100) - \left[\frac{e_{s_{T_c(100)}}}{s}\right] \quad (4)$$

Where $T_c(100)$ is the critical temperature at 100% RH and $T_c(0)$ is the critical temperature at zero percent RH. To find $T_c(40)$, multiply the saturation vapor pressure at $T_c(100)$ by 40% and divide this number by the critical slope. Add the resulting number to $T_c(0)$. This gives the $T_c(40)$shown by Equation 5. Other critical temperatures are obtained in the same way.

$$T_c(40) = T_c(0) + \left[\frac{e_{s_{T_c(100)}} \times .40}{s}\right] \quad (5)$$

Once you calculate critical temperatures for at least four flight levels, you can find the critical temperatures for the remaining flight levels by interpolation. Plot the calculated critical temperatures on a flight-level versus temperature graph and connect the points with a line. The line gives the extrapolated critical temperatures for a given flight level and relative humidity.

8. ENGINE-SPECIFIC ALGORITHM VERIFICATION

The engine-specific algorithms were verified using a subset of the SAC contrail database that was confined to data from B-52G, KC-135A, KC-135R and U-2 aircraft. Table 5 shows the number of observations used to verify the algorithms. The B-52G, KC-135A and U-2 are powered by turbojet engines; the KC-135R, by high-bypass turbofans. Since there was no data for low-bypass turbofans, those algorithms were not verified

TABLE 5. Observations Used to Verify Engine-Specific Algorithms.

	OCCURRENCE	NON-OCCURRENCE	TOTAL
U-2	633	407	1040
KC-135R	127	171	298
KC-135A	143	143	286
B-52G	78	87	165

U-2 pilots provided 1,040 observations from above 40,000 feet; these observations verified the usefulness of the new algorithms at these very high flight levels. Table 6 shows the probability of detection (POD), false alarm rate (FAR) and discriminant "V' score (VDS) for the Appleman method, the non-bypass algorithm, and the 18-hour AFGWC contrail forecast for data above 40,000 feet.

TABLE 6. Non-bypass Algorithm Verification Based on U-2 Data.

	OCCURRENCE		NON-OCCURRENCE		
	POD	FAR	POD	FAR	VDS
APPLEMAN	96%	27%	46%	12%	0.42
NON BY-PASS	75%	11%	86%	31%	0.62
GWC	62%	16%	80%	43%	0.43

Note that the non-bypass algorithm (POD 86%) is much better than the Appleman method (POD 46%) in predicting *non-occurrence* of contrails. Overall, the non-bypass algorithm, with a VDS of 0.62, shows much more skill than the Appleman method (VDS 0.42) and the AFGWC model (VDS 0.43). The non-bypass algorithm, then, is superior to the Appleman method for making U-2 contrail forecasts.

B-52G and KC-135A crews provided a total of 451 contrail observations. Tables 7 and 8 show the verification statistics for these aircraft.

TABLE 7. Non-Bypass Algorithm Verification Based on KC-135A Data.

	OCCURRENCE		NON-OCCURRENCE		
	POD	FAR	POD	FAR	VDS
APPLEMAN	45%	9%	95%	40%	0.40
NON BY-PASS	61%	18%	85%	34%	0.46
GWC	28%	2%	99%	42%	0.27

TABLE 8. Non-Bypass Algorithm Verification Based on B-52G Data.

	OCCURRENCE		NON-OCCURRENCE		
	POD	FAR	POD	FAR	VDS
APPLEMAN	24%	7%	98%	49%	0.22
NON BY-PASS	40%	5%	98%	43%	0.37
GWC	14%	15%	98%	44%	0.12

The non-bypass algorithm is better than the Appleman method for both aircraft types, but the PODs for all methods were much lower than the POD for the U-2. This is probably because of the high variability of relative humidity at flight levels commonly flown by B-52s and KC-135s; 89% of the observations from those two aircraft were recorded at or below 32,000 feet.

Only 7% of the B52G and KC-135A observations are not accounted for by the non-bypass algorithm, compared to 10% not accounted for by the Appleman method. The most probable cause of limited forecast skill for the B-52G and KC-135A algorithm is the 40% relative humidity assumption used for contrail forecasting in the troposphere.

The high-bypass algorithm was verified using 298 observations provided by KC-135R crews. Table 9 shows the verification comparison statistics.

TABLE 9. High-Bypass Algorithm Verification Based on KC-135R Data.

	OCCURRENCE		NON-OCCURRENCS		
	POD	FAR	POD	FAR	VDS
APPLEMAN	35%	4%	99%	37%	0.34
HIGH BY-PASS	71%	22%	82%	24%	0.53
GWC	28%	0%	100%	38%	0.28

The Appleman method was very weak in forecasting occurrences, with a POD of only 35%. Appleman's POD for non-occurrence was 99%, but the FAR was 37%. Statistics for the AFGWC forecast model are similar to those for the Appleman method; both showed little skill (VDS was 0.34 for Appleman, 0.28 for AFGWC)

The high-bypass algorithm, on the other hand, had a POD of 71% for occurrences and 82% for non-occurrences. VDS was 0.53, better than for Appleman and AFGWC. The high-bypass algorithm uses significantly higher critical temperatures than the Appleman method (see Figures 1 and 10). Since the statistics indicate that it is superior to Appleman, the critical temperatures shown in Figure 10 assume added validity.

Lower occurrence POD and VDS for the non-bypass algorithm (KC-135A and B-52G, Tables 7 & 8) are probably due to the arbitrarily constant humidity. Empirical curves seem to support a 60% RH in the troposphere (as opposed to the 40% RH assumption used in all current forecast methods), but *any* moisture assumption severely limits forecasting skill in the middle and upper troposphere where these two aircraft usually operate. The improvement of contrail forecasting in the middle to upper troposphere for aircraft with non-bypass engines will require better relative humidity forecasts or a method that uses synoptic vertical motion characteristics as a substitute for the relative humidity. Chapter 9 reviews the results of using synoptic-scale vertical motion as a contrail forecasting tool.

9. VERTICAL MOTION CORRELATION (Tropospheric data only)

Synoptic-scale vertical motion has an effect on atmospheric humidity. Upward motion results in the lowering of the ambient temperature, which leads to increased relative humidity. Conversely, downward motion results in the *warming* of the ambient air, which leads to a *decrease* in relative humidity. The use of synoptic-scale vertical motion as a contrail forecasting tool is based on this simple argument.

Each observation's location was analyzed for synoptic-scale vertical motion. The sign of the vertical motion was estimated using the 300-mb trough-ridge pattern. Upward motion was assumed to exist between the base of a trough and the apex of the upstream ridge. Downward motion was assumed to exist between the apex of the ridge and the base of the upstream trough.

Four vertical motion forecasting methods were tested; they are shown below. All four used the critical temperature at 40% RH, $T_c(40)$, as a reference point. Verification statistics are given in Tables 10, 11, and 12.

Four "vertical motion" forecasting rules

Method 1. The "2-Degree Rule" - If the temperature is within ±2° C of $T_c(40)$ and there is *upward* motion, forecast contrails; if there is *downward* motion, forecast *no* contrails.

Method 2. The "3-Degree Rule" - If the temperature is within ±3° C of $T_c(40)$ and there is *upward* motion, forecast contrails; if there is *downward* motion, forecast *no* contrails.

Method 3. The "Plus-2 Rule" - If the temperature is within +2° C of $T_c(40)$ and there is *upward* motion, forecast contrails; if there is *downward* motion, forecast *no* contrails.

Method 4. The "Plus-3 Rule" - If the temperature is within +3° C of $T_c(40)$ and there is *upward* motion, forecast contrails; if there is *downward* motion, forecast *no* contrails.

Note: for temperatures higher than $T_c(40)$, forecast *no contrails* regardless of the vertical motion characteristics.

As shown in Tables 10 and 11 below, the 2- and 3-Degree Rules on the preceding page don't improve on the skill of the high-bypass algorithm based on KC-135R data. However, for the B-52G there was an 11% increase in contrail occurrence POD using the 2-Degree Rule and a 15% increase using the 3-Degree Rule (compare Tables 8, 10, and 11). For the KC-135A, all the statistics improved; VDS was slightly better when using the vertical motion rules.

TABLE 10. Verification Statistics for the 2-Degree Rule.

	OCCURRENCE		NON-OCCURRENCE		
	POD	FAR	POD	FAR	VDS
KC-135R	72%	20%	85%	22%	0.57
KC-135A	70%	14%	87%	28%	0.57
B-52G	51%	9%	94%	39%	0.45

TABLE 11. Verification Statistics for the 3-Degree Rule.

	OCCURRENCE		NON-OCCURRENCE		
	POD	FAR	POD	FAR	VDS
KC-135R	75%	21%	74%	31%	0.49
KC-135A	65%	12%	90%	31%	0.49
B-52G	55%	8%	94%	38%	0.49

Tables 12 and 13 show an increase in skill for the B-52G and KC-135A. For example, VDS for the B-52G increases to 0.59 with the Plus-2 Rule and to 0.60 with the Plus-3 Rule; this compares to a VDS of 0.37 for the non-bypass algorithm.

TABLE 12. Verification Statistics for the Plus-2 Rule.

	OCCURRENCE		NON-OCCURRENCE		
	POD	FAR	POD	FAR	VDS
KC-135R	76%	24%	79%	21%	0.56
KC-135A	72%	18%	82%	28%	0.53
B-52G	69%	8%	90%	30%	0.59

TABLE 13. Verification Statistics for the Plus-3 Rule.

	OCCURRENCE		NON-OCCURRENCE		
	POD	FAR	POD	FAR	VDS
KC-135R	80%	27%	75%	19%	0.55
KC-135A	71%	17%	83%	29%	0.54
B-52G	68%	7%	92%	36%	0.60

The KC-135A Plus-2 and Plus-3 Rules showed only small gains in VDS, but both were above 0.50. The much greater improvement in VDS for the B-52G and KC-135A than for the KC-135R when using the Plus-2 or Plus-3 Rule is not surprising; the gradient of relative humidity is greater from $T_c(40)$ to $T_c(100)$ for the non-bypass algorithm than for the high-bypass algorithm. The Plus-2 or Plus-3 Rule will therefore cover a greater range of relative humidities for the non-bypass algorithm than for the high-bypass algorithm.

The results of the vertical motion correlation are encouraging but not conclusive. More work is needed to further refine the use of synoptic-scale vertical motion as a contrail forecasting input variable. More studies using vertical motion forecasts from various models are needed. Forecasters may wish to experiment with various vertical motion rules and engine-specific algorithms given here to improve their contrail forecasts.

Bjornson (1992) applied discriminant analysis to SAC's engine-specific data; this empirical contrail forecasting technique scored much higher than the SAC/DOW technique when using B-52G data, and slightly higher using KC-135R data (see USAFETAC/PR--92/003, Appendix D). There was little difference in the two techniques when using KC-135A or U-2 data. Bjornson postulates that the USAFETAC technique probably produces better results than the theoretical technique because it does not assume an RH for the troposphere or stratosphere.

10. SUMMARY AND CONCLUSIONS

Planners and pilots have been concerned with contrails since World War II. Contrails are visible from the ground as well as from satellites and other aircraft. Since the detection of high-flying aircraft is made easier by visible contrails, accurate contrail forecasting is vital to aircrews seeking to avoid detection.

This study was initiated because of Strategic Air Command concern over the accuracy of contrail forecasts provided to aircrews by the Air Force Global Weather Central. AFGWC's low skill in forecasting contrails was of such great concern because pilots need accurate forecasts of contrail-formation areas to allow flight level and route adjustments to minimize the potential for contrail formation. The study was based on a database consisting of more than 5,400 contrail reports supplied by SAC aircrews flying aircraft powered by modern turbojet and turbofan engines.

The relative skills of the AFGWC 18-hour contrail forecast model and the Appleman method were determined and compared. Both were found to severely underforecast the formation of contrails in the troposphere, with contrail PODs of 24 and 27%, respectively. Since the POD of the Appleman method was only 27%, many SAC aircraft were producing contrails when they should not have. But when using U-2 data, the opposite occurred; The Appleman method's non-occurrence POD was a low 46%. This finding led to the development of engine-specific contrail algorithms.

Engine characteristics data for the most common modern engine types (non-bypass turbojet and low- and high-bypass turbofan) were obtained from United Technologies/ Pratt & Whitney. The exhaust characteristics of moisture and temperature in the tailpipe were evaluated over a range of power settings, Mach numbers, and flight levels New contrail forecast algorithms were developed using this data; they were verified using the B-52G, KC-135A, KC-135R and U-2 data in the new SAC PIREP database. In all cases, the new, easy to use algorithms showed better forecast skill than the Appleman method.

Because the contrail forecasting process uses assumed, rather than actual, relative humidities, accuracy is still limited. To refine contrail forecasts further, accurate observations and forecasts of relative humidity are needed well into the stratosphere. When the moisture (RH) variable is unknown, empirical curves can provide some assistance in contrail forecasting. Data for several types of engines, however, has not yet been collected; until it is, moisture curves for those engines cannot be developed.

Another limitation is the possibility that the new algorithms may not meet specific user requirements because of different engine exhaust characteristics. We have included instructions, therefore, for deriving user-specific contrail forecasting algorithms.

The ability to forecast contrail conditions accurately at different flight levels can significantly improve the weather support you give your customer. On most days, it's likely that your customer will think the contrail forecast of little importance; under hostile conditions, however, when the enemy may rely on visual sighting of aircraft as a supplement to air defense radar, good contrail forecasts will be highly appreciated. An accurate contrail forecast might, in fact, save someone's life.

BIBLIOGRAPHY

Appleman, H.S., "The Formation of Exhaust Condensation Trails by Jet Aircraft," *Bulletin of American Meteorological Society*, Vol 34, pp 14-20, January 1953.

Dobson, G.M.B., *Condensation Trails from Aeroplane Exhaust and Meteorological Conditions*, Gr. Br. Aer. Res. Comm., T.A. 161, 1941.

Bjornson, Brian M., *SAC Contrail Formation Study*, USAFETAC/PR--92/003, USAF Environmental Technical Applications Center, Scott AFB, IL, 1992.

Bohren, Craig F., *Clouds in a Glass of Beer*, John Wiley & Sons, New York, N.Y., 1987.

Duffield, Lt Col G. and Maj G. Nastrom, *Equations and Algorithms for Meteorological Applications in Air Weather Service*, AWS/TR-83/001, HQ Air Weather Service, Scott AFB IL, December 1983.

Goldie, A.H.R., *Formation of Cloud Behind Aircraft*, Gr. Br. Aer. Res. Comm., H.A.S. 42 1941a.

Goldie, A.H.R., *Condensation Trails from Aircraft*, Gr. Br. Aer. Res. Comm., T.4066, 1941b.

Hanssen, A.W., and W.J.A. Kuipers, *On the Relationship Between the Frequency of Rain and Various Meteorology Parameters*, Koninklijk Nederlands Meteorologisch Institu., Med Ed. Verhand., 81, 2-15, 1968

Jiusto, J.E., *Prediction of Aircraft Condensation Trails: Project Contrails*, Report No. VC-1055-P-5, Cornell Aeronautical Laboratory, 1961.

Jiusto, J.E., and R.J. Pilie, *Contrail Forecasting*, CAL Report No. VC-1660-P-3, Cornell Aeronautical Laboratory, 1964.

Lee, T.F., "Jet Contrail Identification using the AVHRR Infrared Split Window," *Journal of Applied Meteorology*, Vol 28, pp 993-995, September 1989.

Miller, W.F., *SAC Contrail Forecasting Algorithm Validation Study*, USAFETAC/PR-90/003, USAF Environmental Technical Applications Center, Scott AFB, IL, 1990.

Rango, A.L., and P.V. Hobbs, "Production of Ice Particles in Clouds due to Aircraft Penetrations," *Journal of Climate and Applied Meteorology*, Vol 22, pp 214-232, 1983.

DISTRIBUTION

HQ AF/XOWR, 1490 Air Force Pentagon, Rm BF866, Washington, DC 20330-1490 . . . 1
HQ USAF/XOOOW, Rm BD927, 5054 Air Force Pentagon, Washington, DC 20330-5054 . . . 1
OSAF/SS, Rm 4C1052, 6560 Air Force Pentagon, Washington, DC 20330-6560 . . . 1
USTC J3/J4-OW, 508 Scott Dr., Bldg 1900, Scott AFB, IL 62225-5357 . . . 1

AWS/XTX/DO/XT , 102 W Losey St., Bldg 1521, Scott AFB, IL 62225-5206 . . . 1
Det 4, Hq AWS, Bldg 91027, 595 Independence Rd, Hurlburt Fld, FL 32544-5618 . . . 1
Det 5, HQ AWS, Wall Studio, Bldg 0902, 709 H St, Ste 201, Keesler AFB MS 39534-2447 . . . 1
OL-B, HQ AWS (ESC/AVD), Hanscom AFB, MA 01731-2816 . . . 1
OL-F, HQ AWS SMC/CIA, PO BOX 92960, 2401 El Segundo Blvd, Los Angeles CA 90009-2960 . . . 1
OL-K, HQ AWS, NEXRAD Ops Support Facility, 3200 Marshall Dr Ste 100, Norman, OK 73072-8028 . . . 1
OL-N, HQ AWS, c/o ARL (AMSRL-BE-W), Bldg 1646 Rm 24, White Sands Missile Rng, NM 88002-5501 . . . 1
OL-M, HQ AWS, SM-ALC/H, 320 Peacekeeper Way Ste 3, McClellan AFB CA 95652-1027 . . . 1

HQ AFGWC/DO/DOM, MBB39, 106 Peacekeeper Dr., Ste 2N3, Offutt AFB, NE 86113-4039 . . . 1
AFSFC/DOM, 715 Kepler Ave, Ste 60, Falcon AFB, CO 80912-7160 . . . 1
USAFETAC, 859 Buchanan St, Scott AFB, IL 62225-5116 . . . 6

USSTRATCOM/J3615, 901 SAC Blvd, Ste 1F14, Offutt AFB, NE 68113-6700 . . . 1
USCENTCOM/CCJ3-W, Bldg 540, MacDill Blvd, MacDill AFB, FL 33608-7001 . . . 1
USSOCCENT/SOCJ2-SWO, 7115 S. Boundary Dr, MacDill AFB, FL 33621-5101 . . . 1
USSOCOM/SOJ3-W, Spec Ops, MacDill AFB, FL 33605-6001 . . . 1

ACC/DOW,30 Elm St, Ste 215, Langley AFB, VA 23655-2093 . . . 1
1 WS/CC, 190 E Flightline Rd, Ste 100, Langley AFB, VA 23665-5508 . . . 1
1 WS/CC, Weather Support Unit, Bldg 693, Rm 203, Langley AFB VA 23665-5000 . . . 1
2 WS/CC, 245 Davis Ave East, Barksdale AFB LA 71110-2269 . . . 1
24WS/CC, Unit 0640, APO AA 34001-5000 . . . 1
46 WS/CC, 601 W Choctawhatchee Ave, Ste 60, Eglin AFB,FL 32542-5719 . . . 1
Det 1, NEADS/DOW, 105 Maineiac Ave., Ste 510, Bangor ANGB, ME 04401-3099 . . . 1
2AF/DRW, 8801 C St, Ste 600, Beale AFB CA 95903-1537 . . . 1
4 OSS/OSW, 1980 Curtiss Ave., Ste 100, Seymour Johnson AFB, NC 27531-2524 . . . 1
5 OSS/DOW, 221 Flight Line Dr., Bldg 746, Minot AFB, MD 58705-5021 . . . 1
7 OSS/DOW, Bldg 1425, Carswell AFB, TX 76127-5000 . . . 1
9COS/AOSW, 524 Shaw Dr, Shaw AFB, SC 29152-5029 . . . 1
9 OSS/DOW, 7800 Arnold Ave Ste 100, Beale AFB, CA 95903-1217 . . . 1
10 OSS/DOW, F Ave., Bldg 401, Ste 7, K.I. Sawyer AFB, MI 49843-3400 . . . 1
12 COS /AOSW, 5325 E Kachina St, Davis-Monthan AFB AZ 85707-4921 . . . 1
22 OSS/DOW, 2645 Graeber St, Ste 3, March AFB, CA 92518-2264 . . . 1
27 OSS/OSW, 110 E Sextant Ave., Ste 1040, Cannon AFB, NM 88103-5322 . . . 1
28 OSS/OSW, 1820 Vandenburg Ct, Ellsworth AFB, SD 57706-4729 . . . 1
42 OSS/DOW, Georgia Rd., Bldg 8200, Rm 10, Loring AFB, ME 04751-5000 . . . 1
43 OSS/DOW, 7224 Flightline Dr, Malmstrom AFB, MT 59402-7526 . . . 1
49 OSS/OSW, Bldg 571, Holloman AFB, NM 88330-5000 . . . 1
55 OSS/DOW, 509 SAC Blvd, Ste 1, Bldg T29, Offutt AFB, NE 68113-2094 . . . 1
56 OSS/OSW, Bldg P3, Rm 101, Florida Ave., MacDill AFB, FL 33608-5000 . . . 1
57 OSS/OSW, 27 Depot Rd., Bldg 805, Nellis AFB, NV 89191-5000 . . . 1
58 OSS/OSW, 8th St., 7254 N. 142 Ave., Ste 3, Luke AFB, AZ 85309-1233 . . . 1
67 OSS/DOMS, Bergstrom AFB TX 78743-5000 . . . 1
90 OSS/DOW, 7505 Saber Rd., Bldg 1250, F.E. Warren AFB, WY 82001-5000 . . . 1
92 OSS/OSW, Bldg 1, Fairchild AFB, WA 99011-5000 . . . 1
93 OSS/DOW, 7th St., Bldg 1340, Castle AFB, CA 95342-5000 . . . 1
96 OSS/DOW, Base Ops Rd., Bldg 9001, Dyess AFB, TX 79607-5000 . . . 1

97 OSS/WXF, 603 E Ave, Ste 1, Altus AFB, OK 73523-5033 1
305 OSS/DOW, Hoosier Blvd, Bldg S-28, Grissom AFB, IN 46971-5000 1
319 OSS/DOW, 695 Steen Ave., Bldg 528, Ste 106, Grand Forks AFB, ND 58205-6244 1
325 OSS/OSW, Stop 22, Tyndall AFB, FL 32403-5048 1
347 OSS/OSW, 8227 Knights Way, Ste 106, Moody AFB, GA 31699-1899 1
355 OSS/OSW, Phoenix St., Bldg 4820, Davis-Monthan AFB, AZ 85707-6801 1
366 OSS/OSS, 655 Oak St., Mt Home AFB, ID 83648-5401 1
380 OSS/DOW, 22 Alabama Ave., Ste 207, Bldg 2712, Rm 100, Plattsburgh AFB, NY 12903-2705 1
384 OSS/DOW, Kansas Ct., Ste 104, Bldg 1112, McConnell AFB, KS 67221-5000 1
416 OSS/OSW, 592 Hangar Rd.,Bldg 100, Ste 121, Griffiss AFB, NY 13441-4520 1
509 OSS/OSW, 745 Arnold Ave, Ste 1A, Whiteman AFB, MO 65305-5026 1

HQ 1st WEAG/WSOT, Bldg 130 Anderson Way, Ft McPherson, GA 30300-5000 1
OL-A, 1st WEAG, Bldg 6212, Ft Irwin, CA 92310-3000 1

AMC/XOW, 402 Scott Dr,. Rm 132, Scott AFB, IL 62225-5363 1
AMC/XOWR, 402 Scott Dr,. Unit 3C1, Scott AFB, IL 62225-5302 1
1 SOW/OGSW. Attn: Lt Kelly, 150 Bennett, Bldg 90730, Hurlburt Fld, FL 32544-5000 1
23 OSS/OSW, 1427 Surveyor St, Ste A, Pope AFB NC 28308-2797 1
60 OSS/WX, 401 2d St, Bldg P4, Travis AFB, CA 94535-5986 1
62 OSS/WXF, 1172 E St, McChord AFB, WA 98438-1008 1
63 OSS/OSW, Bldg 795, Norton AFB, CA 92409-5987 1
89 OSS/WX, 1240 Menoher Dr, Bldg 1220, Andrews AFB, MD 20331-6511 1
97 OSS/WXF, 603 E Ave, Ste 1, Altus AFB, OK 73523-5033 1
23OSS/OSW, Bldg 708, Pope AFB, NC 28308-5000 1
314 OSS/OSW, 2740 First St., Bldg 120, Little Rock AFB, AR 72099-5060 1
375 WS/OGWB, 433 Hangar Rd, Rm 139, Scott AFB, IL 62225-5029 1
377 ABW/OTW, 3400 Clark Ave, Kirtland AFB, NM 87117-5776 1
436 OSS/WXF, 501 Eagle Way, Ste B, Bldg 501, Dover AFB, DE 19902-7504 1
437 OSS/SSW, 101 S. Bates, Ste A, Bldg 162, Charleston AFB, SC 29404-5013 1
438 OSS/WXF, Bldg 1730, Vandenberg Ave., McGuire AFB, NJ 08641-5509 1

HQ AFSPACECOM/DOGW, 150 Vandenberg St, Ste 1105, Peterson AFB, CO 80914-4200 1
21 OSS/OGSW, Hamilton Rd., Stop 22, Peterson AFB, CO 80914-5000 1
721 SPTS Weather, Ste 2-210, 1 Norad Rd, Cheyenne Mtn, CO 80914-6113 1
45 WS, Bldg 423, C. St., Patrick AFB, FL 32925-6537 1
AFTAC/DOW, Patrick AFB, FL 32925-5000 2
30WS, Coral Rd., Bldg 21150, Vandenberg AFB, CA 93437-5000 1
SSD/IMO, PO Box 92960, Los Angeles, CA 90009-2960 1
SMC/SDEW, 160 Skynet St Ste 2315 Los Angeles AFB CA 90245-4683 1
SMC/CIA, 2420 Vela Way Suite 1467 D 9, Los Angeles AFB, CA 90245-4659 1
Det 2, SMC/TDOR (Weather), Onizuka AFB, 1080 Lockheed Way, Box 044, Bldg 1001, Sunnyvale CA 1
OD 4/DX, Onizuka AFB, CA 94088-3430 1
SSD OD 4, Onizuka AFB, CA 94088-3430 1
Det 3, Space Systems, Bldg 430, Stop 77, Buckley ANGB, CO 80011-9599 1
NASA-MSFC-ES44, Attn: Dale Johnson, Huntsville, AL 35812- 000 1
NASA-MSFC-ES44, Attn: Gwenevere Jasper, Huntsville, AL 35812-5000 1

AFMC/DOW, 4225 Logistics Ave, Ste 2, Wright-Patterson AFB OH 45433-5714 1
645 WS/DO. 5291 Skeel Ave, Ste 1, Wright-Patterson AFB, OH 45433-5231 1
FASTC/TAW, 4115 Hebble Creek Rd., Ste 33, Wright-Patterson AFB, OH 45433-5637 1
AS[illegible]E, Bldg 91, 3rd St, Wright-Patterson AFB, OH 45433-6503 1
AF[illegible]IR, Wright-Patterson AFB, OH 45433-6583 1
W[illegible]DA, Wright-Patterson AFB, OH 45433-6543 1
WL/DOW, Bldg 22 2690 C St Ste 2, Wright Patterson AFB, OH 45433-6543 1
WL/WEM, Wright-Patterson AFB OH 45433-2563 1

WRDC/WE, Wright-Patterson AFB OH 45433-6543 1
UTTR/WE, Hill AFB, UT 84056-5000 1
AFOTEC/WE, Kirtland AFB, NM 87117-7001 1
ESMC/WE, Patrick AFB, FL 32925-5000 1
ESC/WE, 5 Eglin St, Hanscom AFB, MA 01731-2122 1
PL/GP, Hanscom AFB, MA 01731-5000 1
PL/TSML, 5 Wright St, Hanscom AFB MA 017313004 1
PL/WE, Kirtland AFB, NM 87117-5987 1
AFCESA/WE, Tyndall AFB, FL 32403-5000 1
AFESC/RDXT, Bldg 1120, Stop 21, Tyndall AFB, FL 32403-5000 1
46 TG/WE, Holloman AFB, NM 88330-5000 1
325 OSS/OSW, Florida Ave., Stop 22, Bldg 149, Tyndall AFB, IL 32403-5048 1
AFFTC/WE, Edwards AFB, CA 93523-5000 1
412 OSS/WE, 85 South Flightline Rd., Edwards AFB, CA 93524-6460 1
510 OSS/WE, Bldg 1200, Rm 6, Wolfe Ave, Edwards AFB, CA 93523-5000 1
OL-A, AFCOS, Site R, Fort Ritchie, MD 21719-5010 1
USAFALCENT RA, Pope AFB, NC 28308-5000 1
CCSO/FL, Tinker AFB, OK 73145-6340 1
304 ARRS/DOOR, Portland IAP, OR 97218-2797 1
AFOSR/NL, Bolling AFB, DC 20332-5000 1
TFWC/WE, Nellis AFB, NV 89191-5000 1
AL/OEBE, 2402 East Drive, Brooks AFB, TX 78235-5114 1

AETC/XOSW, 1F St Ste 2, Randolph AFB, TX 78150-4325 1
AU/WE, 55 LeMay Plaza S., Maxwell AFB, AL 36112-6335 1
334 TTS/TTMV, Bdlg 4342, 700 H St, Keesler AFB, MS 39534-2499 2
Cape Canaveral Forecast Facility,/ROCC, Bldg 81900, Cape Canaveral AFS FL 32925-6537 1

5 WS (PACAF), Unit 15173, APO AP 96205-0108 1
Det 1, 5 WS, Unit 15678, APO AP 96205-0678 1
OSS/WS, Unit 2139, APO AP 96264-2139 1
603 ACCS/WE, Unit 2051, APO AP 96278-2072 1

PACAF/DOW, Bldg 1102, 25 E St, Ste I232, Hickam AFB, HI 96853-5426 1
15 WS, 800 Hangar Ave, Hickam AFB HI 96853-5244 1
Det 1, 15WS, 1102 Wright Ave, Wheeler AAF HI 96854-5200 1
18 OSS/OSW, Unit 5177, Box 10, APO AP 96368-5177 1
374 OSS/DOW, UNIT 5222, APO AP 96328-5222 1
OL-A, 374 OSS, APO AP 96343-0085 1
432 OSS/OGSW, Unit 5011, APO AP 96319-5011 1

623 SPTS/DOW, Unit 12503, APO AP 96510-2503 1
643 SPTS/OF, Unit 12526, APO AP 96513-2526 1
673 OPS/WE, Unit 12509, APO AP 96512-2250 1

11 OPG/WE, 6900 9th Ste 205, Elmendorf AFB, AK 99506-5000 1
3 OSS/WE, 7th St., Bldg 32235, Elmendorf AFB, AK 99506-5000 1
343 WS, 1215 Flightline Ave, Ste 2, Eielson AFB, AK 99702-1520 1
Det 1, 343 WS, Ft Wainwright, AK 99703-5200 1
633 OSS/OSW, Unit 14035, APO AP 96543-4035 1
Det 1, 633 OSS, COMNAVMAR, PSC 489, Box 20, FPO AP 96536-0051 1

HQ NATO Staff Meteorological Officer IMS/OPS APO AE 09724 1
USAFE/DOW, Unit 3050, Box 15, APO AE 09094-5015 1
USAFE/DOWO, Unit 3050, Box 500, APO AE 09094-5015 1
17AF/WE, Unit 4065, APO AE 09136-5000 1

86 OPS GP, Unit 8495, APO AE 09094-5015 . . . 1
Det 1, 86WS (USAFE), Unit # 7890, APO AE 09126-7890 . . . 1
10 TFW/DOM, Unit 5685, PSC #47, APO AE 09470-5000 . . . 1
20 OSS/DOM, Unit 5475, APO AE 09466-5000 . . . 1
32 OSS/WE, Unit 6795, APO AE 09719-5000 . . . 1
36 OSS/WE, Unit 3860, APO AE 09132-5000 . . . 1
39 OSS/OSW, Unit 7090, Box 115, APO AE 09824-5000 . . . 1
48 OSS/DOM, Unit 5245, Box 390, APO AE 09464-5390 . . . 1
52 OSS/WEF, Unit 8870, Box 270, APO AE 09126-0270 . . . 1
65 ALSS/WEF, APO AE 09720-7795 . . . 1
86 WF, Unit 3090, APO AE 09094-5000 . . . 1
100 OSS/DOW, Unit 4965, APO AE 09459-5000 . . . 1
401 OSS/OGSW, Unit 6160, APO AE 09601-5000 . . . 1
435 OSS/DOW, Unit 7435, APO AE 09097-5000 . . . 1

7WS, Unit 29351, APO AE 09014-5000 . . . 1
Det 1, 7WS, HQ USEUCOM ECJ3-OD-WE, Unit 30400 Box 1000, APO AE 09128-5000 . . . 1
Det 2, 7WS, Unit 20200, APO AE 09165-9816 . . . 1
Det 3, 7WS, Unit 29231, APO AE 09102-3737 . . . 1
Det 6, 7WS, Cmr 453, APO AE 09146-0979 . . . 1
Det 7, 7WS, Unit 28130, APO AE 09114-5000 . . . 1
Det 8, 7WS, Unit 25202, APO AE 09079-5000 . . . 1
Det 10, 7WS, Unit 26410, APO AE 09182-0006 . . . 1
Det 13, 7WS, Cmr 416, Box S, APO AE 09140-9998 . . . 1
Det 26, 7WS, Unit 29632, APO AE 09096-5000 . . . 1

105 Weather Flight, Tennessee Air National Guard, PO Box 17267, Nashville, TN 32717-0267 . . . 1
107 Weather Flight, Selfridge ANGB, MI 48045-5024 . . . 1
110 Weather Flight, 10800 Natural Bridge Rd, Bridgeton, MO 63044-2371 . . . 1
111 Weather Flight, Ellington ANGB, TX 77034-5586 . . . 1
113 Weather Flight, IN ANG, Hulman Fld, Terre Haute, IN 47803-5000 . . . 1
116 Weather Flight, WA ANG, Bldg 304, McChord AFB, WA 98433-5000 . . . 1
120 Weather Flight, Buckley ANGB, CO 80011-9599 . . . 1
121 Weather Flight, Stop 28, Andrews AFB, MD 20331-6539 . . . 1
122 Weather Flight, New Orleans NAS, LA 70143-0200 . . . 1
123 Weather Flight, Portland IAP, OR 97218-2797 . . . 1
125 Weather Flight, PO Box 580340, Tulsa AFS, OK 74158-0340 . . . 1
126 Weather Flight, WI ANG, 350 E College, Milwaukee, WI 53207-6298 . . . 1
127 Weather Flight, Forbes Fld, Topeka, KS 66619-5000 . . . 1
130 Weather Flight, Yeager Apt, Charleston, WV 25311-5000 . . . 1
131 Weather Flight, Barnes Map, Westfield, MA 01085-1385 . . . 1
140 Weather Flight, Willow Grove NAS, PA 19090-5105 . . . 1
146 Weather Flight, GTR Pittsburg ANG AN, PA 15231-0459 . . . 1
154 Weather Flight, Camp Robinson, North Little Rock, AR 72118-2200 . . . 1
156 Weather Flight, 5225 Morris Fld Dr., Charlotte, NC 28208-5797 . . . 1
159 Weather Flight, c/o HQ FLANG, State Arsenal, St Augustine, FL 32085-1008 . . . 1
164 Weather Flight, Rickenbacker ANGB, OH 43217-5007 . . . 1
165 Weather Flight, Standiford Fld, Louisville, KY 40213-2678 . . . 1
181 Weather Flight, 8150 W Jefferson Blv, Dallas, TX 75211-9570 . . . 1
195 Weather Flight, 4146 Naval Air Rd., Port Huenene, CA 93041-4001 . . . 1
199 Weather Flight, 1102 Wright Ave, Hickam AFB, HI 96853-5200 . . . 1
200 Weather Flight, 5680 Beulah Rd., Sandston, VA 23150-6109 . . . 1
202 Weather Flight, Otis ANGB, MA 02542-5028 . . . 1
203 Weather Flight, Ft Indiantown GAP, Annville, PA 17003-5002 . . . 1
204 Weather Flight, McGuire AFB, NJ 08641-6004 . . . 1
207 Weather Flight, 3558 N. Michigan Rd., Shelbyville, IN 46176-4914 . . . 1

208 Weather Flight, 206 Airport DE, St Paul, MN 55107-4098 1
209 Weather Flight, PO Box 5218, Austin, TX 78763-5218 1

COMNAVOCEANCOM, Code N312, Stennis Space Ctr, MS 39529-5000 2
COMNAVOCEANCOM (Capt Brown, Code N332), Stennis Space Ctr, MS 39529-5001 1
NAVOCEANO (Barnie Rau), Code OISE, Bldg 8100, Rm 203D, Stennis Space Ctr, MS 39522-5001 2
NAVOCEANO (Tony Ortolano), Code 9220, Stennis Space Ctr, MS 39529-5001 1
Maury Oceanographic Library, Naval Oceanography Office, Stennis Space Ctr, MS 39522-5001 1
Naval Research Laboratory, Monterey, CA 93943-5006 1
Naval Research Laboratory, Code 4323, Washington, DC 20375 1
Naval Postgraduate School, Chmn, Dept of Meteorology, Code 63, Monterey, CA 93943-5000 1
Naval Air Warfare Center-Weapons Division, Geophysical Sciences Branch, Code 3254,
Attn: Mr. Roger Helvey, Point Mugu, CA 93042-5001 1

Army Training and Doctrine Command, ATDO-IW (ATTN: SWO), Ft Monroe VA 23651-5000 1
CDR USASOC, Attn: AOIN-ST, Ft Bragg, NC 28307-5200 1
JSOC/Weather, P.O. Box 70239, Ft Bragg, NC 28307-5000
Army Research Lab Battlefield Environment Dir, ATTN: AMSRL-BE-W, White Sands
Missile Range, NM 88002-5501 1
USA TECOM, ATTN: AMSTE-TC-AA (MacBlain), White Sands Missile Range, NM 88002-5504 1
USA TECOM, ATTN: AMSTE-TC-AM (WS), White Sands Missile Range, NM 88002-5501 1
USA TECOM, ATTN: AMSTE-TC-AM CAB, Aberdeen Proving Ground, MD 21005-5001 1
USA TECOM, ATTN: AMSTE-TC-AM (RE) Met Team, Redstone Arsenal, AL 35898-8052 1
USA TECOM, ATTN: AMSTE-TC-AM(BE), c/o NVESD, Ft Belvoir VA 22060-5677 1
USA TECOM, ATTN: AMSEL-RD-NV-VMD (MET), Ft Belvoir VA 22060-5677 1
Director, USA-CETEC, ATTN: GL-AE (Whitmarsh), Fort Belvoir, VA 22060-5546 1
USAIC/SWO, Attn: ATSI-CDW, Ft Huachuca, AZ 85613-6000 1

NCDC Library (D542X2), Federal Building, Asheville, NC 28801-2723 (2 copies of SCSs) 1
PL/TSML, Research Library, Hanscom AFB, MA 01731-5000 1
USAF Rome Lab Tech Lib, FL2810, Corridor W., Ste 262, RL/SUL, Doc Lib, 26 Electronics
Parkway , Bldg 106, Griffiss AFB, NY 13441-4514 1
Technical Library, Dugway Proving Ground, Dugway, UT 84022-5000 1
NOAA/MASC Library MC5, 325 Broadway, Boulder, CO 80303-3328 2
NOAA Library-EOC4W5C4, Attn: ACQ, 6009 Executive Blvd, Rockville, MD 20852 1
NOAA/NESDIS (Attn: Nancy Everson, E/RA22), World Weather Bldg, Rm 703, Washington, DC 20233 1
NGDC, NOAA, Mail Code E/GC4, 325 Broadway, Boulder, CO 80333-3328 1
NWS W/OSD, Bldg SSM C-2 East-West Hwy, Silver Spring, MD 20910 1
NIST Pubs Production, Rm A635, Admin Bldg, Gaithersburg, MD 20899 1

USAFA/DFP, Attn: Capt Paul Bellaire, Colorado Springs, CO 80840-5701 1
DTIC-FDAC, Cameron Station, Alexandria, VA 22304-6145 2
AUL/LSE, Maxwell AFB AL 36112-5564 1
AWSTL, Scott AFB, IL 62225-5438 35